PLOS ONE

RESEARCH ARTICLE

Interference mitigation in intentional jammers aided non-uniform heterogeneous cellular networks

Saleh Mohammed Ghonaim[1☯], Samar Khan[2☯], Faisal Althobiani[3☯], Shadi Alghaffari[4☯], Sheraz Khan[2☯], Muhammad Irfan[5☯], Muhammad Sajid Haroon[6☯], Fazal Muhammad[2☯*]

1 Nautical Science Department, Faculty of Maritime, King Abdulaziz University, Jeddah, Saudi Arabia, **2** Department of Electrical Engineering, University of Engineering and Technology, Mardan, Pakistan, **3** Marine Engineering Department, Faculty of Maritime, King Abdulaziz University, Jeddah, Saudi Arabia, **4** Port and Marine Transportation Department, Faculty of Maritime, King Abdulaziz University, Jeddah, Saudi Arabia, **5** Electrical Engineering Department, College of Engineering, Najran University, Najran, Saudi Arabia, **6** Telecommunications and Networking (TeleCoN) Research Lab, GIK Institute of Engineering Sciences and Technology, Topi, Pakistan

☯ These authors contributed equally to this work.
* fazal.muhammad@uetmardan.edu.pk

Citation: Ghonaim SM, Khan S, Althobiani F, Alghaffari S, Khan S, Irfan M, et al. (2023) Interference mitigation in intentional jammers aided non-uniform heterogeneous cellular networks. PLoS ONE 18(6): e0287709. https://doi.org/10.1371/journal.pone.0287709

Editor: Khalid Taher Mohammed Al-Hussaini, Thamar University: Dhamar University, YEMEN

Received: April 6, 2023

Accepted: June 9, 2023

Published: June 28, 2023

Data Availability Statement: All relevant data are within the paper.

Funding: This research work was funded by Institutional Fund Projects under grant no. (G:138-980-1443). Therefore, authors gratefully acknowledge the technical and financial support from the Ministry of Education and King Abdulaziz University, DSR, Jeddah, Saudi Arabia.

Competing interests: The authors have declared that no competing interests exist.

Abstract

Coverage and capacity are optimized in fifth generation (5G) networks by small base station (SBS) distribution in the coverage realm of macro base station (MBS). However, system performance is significantly reduced by inter-cell interference (ICI) because of the orthogonal frequency division multiple access assumption. In addition to ICI, this work considers intentional jammers' interference (IJI) due to the presence of jammers. These Jammers try to inject undesirable energies into the legitimate communication band, which significantly degrade uplink (UL) signal-to-interference ratio (SIR). To reduce ICI and IJI, in this work, we employ SBS muting, where the SBSs near MBS are switched off. To further mitigate ICI and IJI, we use one of the effective interference management schemes a.k.a reverse frequency allocation (RFA). We presume that due to mitigation in ICI and IJI, the UL coverage performance of the proposed network model can be further improved.

1 Introduction

1.1 Motivation

Heterogeneous cellular networks (HetNets) is a promising candidate technology for the future fifth generation (5G) networks [1–3]. The world wireless research forum predicts high speed connectivity for trillion of devices in the near future [4]. 5G networks can achieve capacity of 100 Gbps with improved battery life, higher coverage, and enhanced user accommodation [5, 6]. HetNets are made up of tiny, small base stations (SBS) coupled with high-power macro base stations (MBS) from a homogeneous cellular network [2, 7]. The deployment of such base stations (BSs) enhances network scalability [8, 9].

Intra-cell interference(ICI) is still the key limiting factor in HetNets despite the adoption of orthogonal frequency division multiple access (OFDMA), which results in minimal intra-cell interference [10, 11].

The functioning of the HetNet network can be negatively impacted by severe intentional jammers' interference (IJI) caused by jammers' presence [12–14]. The location of base stations transmit power, and other network parameters are all presumptively known to such jammers [13]. Therefore, by introducing undesired energy in the appropriate communication range, they can significantly degrade the uplink (UL) signal-to-interference ratio (SIR) [13]. Due to (i) decreased MBS-edge user (M-EU) power transmission in UL, (ii) greater M-EU user distances, and (iii) a higher path-loss exponent, IJI is effective in UL [14, 15].

SBS muting is taken into consideration in HetNets because I a user receives more coverage close to the MBS [5] and (ii) a higher MBS transmit power causes significant co-tier interference [16]. Due to less SBS deployment, SBS muting results in lower ICI and IJI, which enhances network coverage [17].

We refer to SBS muting by non-uniform HetNets (NUHs) and without SBS muting by uniform HetNets (UHs) in the remaining sections of the work. Different interference mitigation strategies, including reverse frequency allocation (RFA) [18], cell range extension (CRE)(CRE) [19], and fractional frequency reuse (FFR) [20], are used in the state-of-the-art. RFA is regarded as one of these plans' proactive and effective interference mitigation strategies [18, 21].

Different key 5G technologies with their applications are presented in [22, 23]. Latest work on HetNets along with emerging technologies, such as (i) non-orthogonal multiple access (NOMA), (ii) massive multiple input multiple outputs (massive MIMO), and (iii) millimeter wave can be found in [24–26].

The works in [27, 28] evaluate both intra-cell interference and ICI in 5G networks. The authors used inter-cell interference coordination (ICIC) technique to mitigate the interference. Through results, it is shown that ICIC leads to improved network performance results. Similarly, in [29], the authors investigate the inter-block interference (IBI) and ICI in HetNets. They propose a novel precoding scheme to reduce ICI and IJI in HetNets.

Their proposed model leads to significant performance superiority due to lower IJI and ICI. The above-mentioned work, however, lacks to investigate both SBS muting and RFA scheme.

The work in [30] study the security aspects of 5G networks focusing on various types of attacks and security services. Moreover, security concerns are evaluated for different 5G technologies, such as software-defined networks, device-to-device communications, heterogeneous networks, massive MIMO, and the Internet of things. Moreover, attacks on 5G networks including traffic analysis, eavesdropping, denial of service, distributed denial of service, and jamming are investigated. The study in [31], provides an in-depth analysis of different jamming and anti-jamming techniques in 5G networks. Similarly, the works in [32] investigate the spoofing and jamming of the physical downlink and UL control channels and signals in 5G networks. Moreover, they employ various jamming methods to evaluate network immunity against jamming. They conclude that effective measures are needed to mitigate jamming in 5G networks. In contrast to our work, [30–32] lacks the employment of RFA and SBS muting to reduce ICI and IJI.

In [33], the authors employ NOMA enabled NUH, where SBSs are distributed with different densities in various regions. Through results, they demonstrate that NOMA-enabled NUH outperforms all other scenarios in terms of energy efficiency. Similarly, the works in [34, 35] explore the employment of NUHs. Their results indicate significant performance improvement due to lower interference achieved by SBS muting in HetNets. However, the latest work of [33–35] lacks to analyze IJI in HetNets.

The latest work on RFA employment can be found in [17, 21, 36], where RFA scheme leads to better coverage and rate due to effective mitigation of interference. However, they lack to investigate both NUH and intentional jammers in HetNets.

In this work, we look into HetNets' performance in terms of coverage when there is IJI and ICI. To alleviate the impact of ICI and IJI we use SBS muting as well as RFA as a preventive measure for interference mitigation.

1.2 Approach and contributions

The paper uses two layers of BS, known as MBSs and SBSs, to illustrate a model based on HetNets. IJI attacks frequently result in additional UL intersections in addition to the typical ICI. Thus, the system as a whole is considered degenerative. In Fig 1A and 1B. the network models are displayed. The MBS service area is divided into two sections: the inner zone, designated A_1, and the edge region, designated A_2, with radii Δs_1 and Δs_2, accordingly [37, 38].

The significance of this work from the state-of-the-art can be summarized as follow.

1. The work in [27–29] evaluates both intra-cell interference and ICI in 5G networks. However, they lack to investigate IJI.
2. In contrast to our work, [30–32] lacks the employment of RFA and SBS muting to reduce ICI and IJI.
3. The latest work of [33–35] evaluates NUHs but lacks to analyse IJI in HetNets.
4. The latest work on RFA employment can be found in [17, 21, 36]. However, they lack to investigate both NUH and IJI in HetNets.

The following are this paper's significant contributions.

1. Analysis of the UL coverage for the typical user which is defined as Slivnyak theorem states that the statistical characteristics of an independent homogeneous Poission Point Process (IHPPP) are preserved and simplified by a typical user at origin [39, 40]., $\mathbb{U}$, in A_2 when IJI and ICI are present.

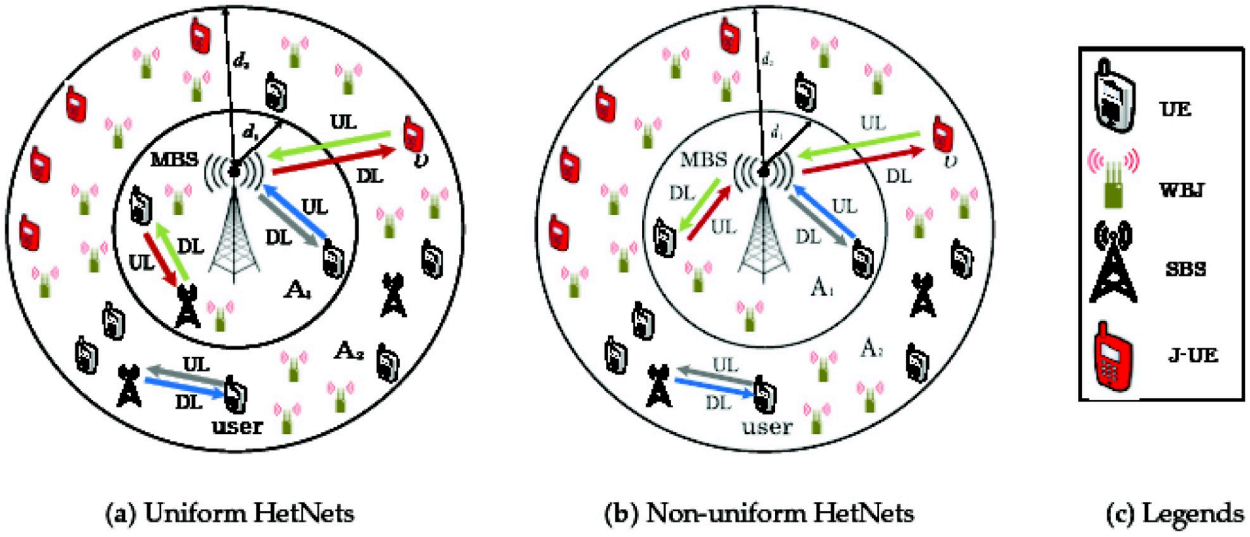

Fig 1. The proposed framework of HetNet that incorporates. A: Uniform HetNets. B: Non-uniform HetNets. C: Legends.

https://doi.org/10.1371/journal.pone.0287709.g001

2. This study examines how proactive interference control strategies can reduce IJI and ICI. RFA and the use of NUHs, a smart network design technique.
3. For (i) UHs with RFA employment (see (10)) and (ii) NUHs with RFA employment (see (11)), we develop coverage probability expressions.
4. The outcomes are presented for various network characteristics, including SIR threshold, jammers' density and transmitted power, users' transmit power and density of SBS.

1.3 Paper organization

The remainder of the paper is laid out as follows. The system model is presented in Section 2. The suggested model's coverage probabilities are calculated in Section 3. Section 4 contains the results and commentary. The paper is finished in Section 5. Table 1 showcases a qualitative tabulation of various references that carried work based on our proposed work that needs improvements while, Table 2 contains an index of the notations made in the article. And finally, Table 3 has the system parameters defined.

2 System model

This section presents the suggested network design as shown in Fig 1A and 1B. Due to multi-tier BSs deployment and the existence of intentional jammers the network performance degrades severely due to ICI and IJI. UL communication of M-EUs in HetNets are susceptible to IJI and ICI because of lower UL transmit power and longer transmission distances between MBS and M-EUs. Moreover, we incorporate RFA in NUH with non uniform BSs deployment to mitigate both ICI and IJI and thus, enhance UL performance of M-EUs. Preliminary mathematical results obtained in this section are used for coverage probability assessment in Section 3.

Table 1. Qualitative reference table.

S.No.	Reference	Methodology	Technique	Benefits	Drawbacks
1	[12]	Heterogeneous Wireless network model (HWNs)with nodes of each tier are located and deployed in PPP with intensities known.	Expressions are derived for random multitier HWNs where joint blackhole jamming attacks exist.	Detection and avoiding association of end users with malicious nodes such as jammers and blackholes.	5G is susceptible to jamming attacks leading to legitimate user coverage interference.
2	[13]	Key parameters of 5G are discussed especially various channels and exchanges between signals over equipment and base stations.	Jamming attack detection such as packet delivery and drop ratios etc., while using the threshold of the defined metrics.	Jamming attack mitigation through frequency hopping spread spectrum(FHSS) and direct sequence spread spectrum (DSSS).	DSSS is capable of achieving protection of high degrees.
3	[14]	Adaptive bias configuration strategy is presented for range extension (RE) through cell load balancing.	Dynamic adaptive bias value is set in accordance to the environmental changes.	RE has the potential to avail low-powered node resource efficiently as well as effectively through cell edge performance.	If bias value is not set properly, interference may increase.
4	[15]	Decoupling association (DeCA) is used for MBS M-EUs to improve UL SIR.	DeCa with RFA	Wide-band jammer (WBJ) cluster severely reduces the UL communication.	Jammer density and transmit power degrades network.
5	[16]	Ground-to-air offloading and BS coordination scheme to enhance mobile users (MUs) performance.	Network throughput, Average spectral efficiency (SE), and analysis through a theoretical framework.	Simulations and numerical analysis validate the impact of key system parameters on system performance demonstrating UAV-assisted offloading scheme advantages.	Flying UAVs require a power source.
Our Work	[39]	RFA in NUH with non-uniform BSs deployment.	RFA	ICI and IJI mitigation to enhance UL performance of M-EU's.	Wastage of SBS resources and system performance degrades due to OFDMA.

https://doi.org/10.1371/journal.pone.0287709.t001

Table 2. Notation summary.

Notation	Description
ϕ_M, ϕ_S, ϕ_j	IHPPPs of MBSs, SBSs, and jammers, respectively
v	Typical user
Γ_M	SIR threshold for MBS
Δs_1, Δs_2	Radii of A_1 and A_2, respectively
$P_{t,v}^{UL}$	UL transmit power of v
ζ_M, ζ_S, ζ_j	Densities of uniformly distributed MBSs, SBSs and jammers, respectively
α	Path loss exponent, $\forall\ \alpha_M = \alpha_S = \alpha$ and $\alpha > 2$
$\lvert h_l\rvert$, $\lvert h_k\rvert$, $\lvert h_j\rvert$	Power gain Rayleigh fading of MBS, SBS and jammers, respectively
r_l, r_k, r_j	distances from MBSs, SBSs, and jammers, respectively $\forall\ l \in \{\phi_M\}$, $k \in \{\phi_S\}$, and $j \in \{\phi_j\}$
SIR_M^{UL}	Uplink SIR received by MBS
UL, DL	Uplink and Downlink, respectively
$\mathcal{L}$	Laplace transform parameter
η_1	Ratio of $P_{t,S}^{DL}$ and $P_{t,v}^{UL}$
η_2	Ratio of $P_{t,j}$ and $P_{t,v}^{UL}$

https://doi.org/10.1371/journal.pone.0287709.t002

Table 3. Simulation parameters.

Parameter	Configuration
MBS, SBS, and IJs	IHPPP
Channel bandwidth	10 MHz
No. of iterations in simulation	10000
Δs_1, Δs_2	600 and 1000 m, respectively
ζ_S	$90 / \pi(500m)^2$ [35]
ζ_M	$3 / \pi(500m)^2$ [39]
ζ_j	$15 / \pi(500m)^2$ [39]
$P_{t,M}^{DL}$, $P_{t,S}^{DL}$, $P_{t,J}$, $P_{t,u}^{UL}$	40 dBm, 30 dBm, 20 dBm and 20 dBm, respectively [48]
$\alpha_m = \alpha_s = \alpha$	$2 < \alpha \leq 4$ [49]

https://doi.org/10.1371/journal.pone.0287709.t003

2.1 Network layoutS

In this paper, we consider two-tier HetNet comprising of co-deployed SBS's with MBS's. We suppose that there exist intentional jammers throughout the network which degrade the desired communication link. MBS's, SBS's, users, and jammers are distributed via IHPPPs ϕ_M, ϕ_S, ϕ_u, and ϕ_J, respectively [17]. The density of MBSs, SBSs, users, and jammers is ζ_M, ζ_S, ζ_u, and ζ_J, respectively. The proposed network models are presented in Fig 1A and 1B [17, 18, 33]. We assume that the UL communication of M-EUs are stressed by IJI and ICI. This work assumes NUHs with RFA in contrast to UHs with RFA to reduce ICI and IJI. Moreover, we investigate the UL coverage performance of $\mathbb{U}$ located in A_2. The path loss exponent is denoted by α [41, 42]. The Rayleigh fading gain, i.e., $|h|^2 \sim \exp(1)$ [17, 40] is represented by $|h|$. For RFA and NUH employment, we divide the MBS coverage region in to A_1 and A_2 with radii Δs_1 and Δs_2, respectively [37, 43].

2.2 Jamming mechanism

Jammers are considered to transmits unwanted energy across the entire spectrum of the communication system to reduce network performance [37, 38, 44]. This work assumes that the

jammers are located uniformly in the coverage vicinity of MBS which are distributed according to IHPPP [35, 45]. The UL communications of M-EUs in HetNet is significantly degraded by ICI and IJI [39]. Due to power constraints, jammers in lower density or located at far distance merely cause any harm to the communication system [15]. Therefore, such low power jammers to be effective, they must be well tuned and need to be located near the target [45, 46]. Moreover, in worst case scenario, jammers block the UL communication in HetNets and, thus, cause the distributed denial of service (DDoS) attacks [39, 45].

2.3 Reverse frequency allocation

Due to efficient interference mitigation, RFA-based resource partitioning significantly improves coverage [39]. By using RFA, the entire spectrum is left open for an SBS to use in the opposite direction and in non-overlapping regions [18, 39]. Various sub-bands are used interchangeably among SBSs and MBSs while following RFA as $A_l^g \; \forall \; g \in (1, 2)$ and $l \in$ (M, S) used alternatively. Fig 2 showcases this scenario. M stands for MBS, while S stands for SBS.

In-accordance with RFA, total alloted frequency band, F, is further divided into sub-bands with different frequencies, i.e., F_1 and F_2, such that $F = \bigcup_{z\in(1,2)} F_z$, as shown in Fig 2. Whereas, these sub-bands F_1 and F_2 of MBS is used for UL and DL communication in outer area macro cell (A_M^2) and inner area of macro cell (A_M^1), respectively. For the UL and DL communication, these sub-bands are further split into UL and DL sub-carriers which are modeled as $F_1 = F_{1,UL} + F_{1,DL}$ and $F_2 = F_{2,UL} + F_{2,DL}$, respectively. Similar to F_1 and F_2, as sub-band frequencies of

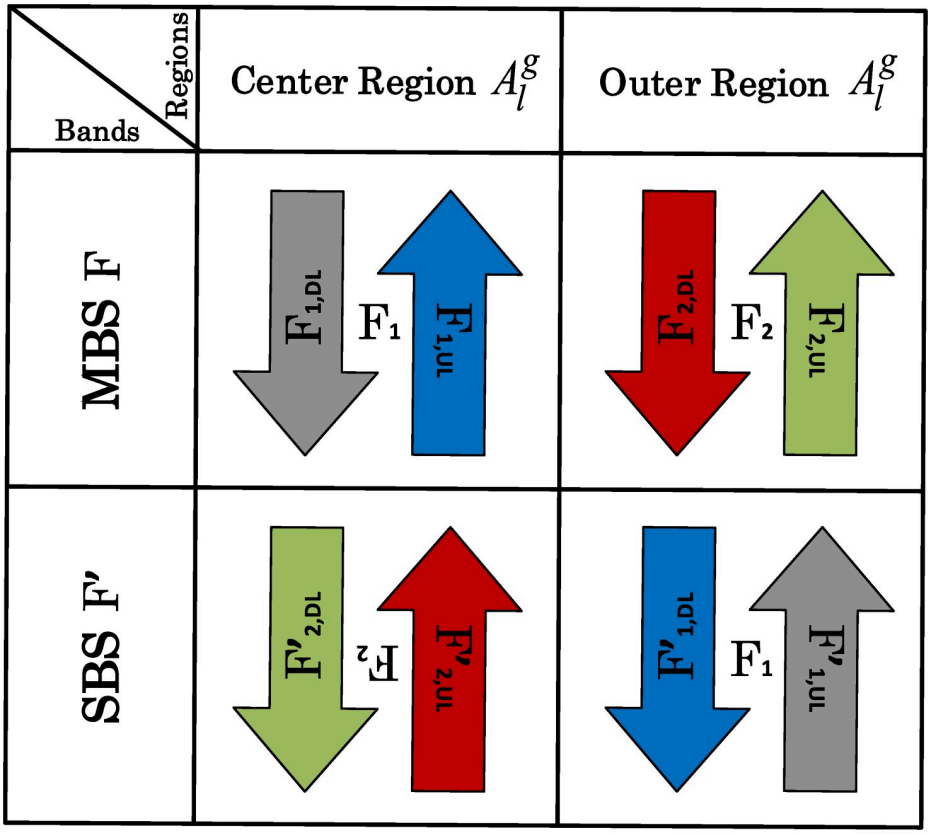

Fig 2. RFA architecture in HetNets.

https://doi.org/10.1371/journal.pone.0287709.g002

MBS, the sub-bands for SBSs are F'_1 and F'_2, respectively, which are reversely used in the corresponding regions reciprocally, i.e., outer region of SBS, A^2_S, and center region of SBS, A^1_S, respectively. These sub-bands of SBSs i.e., F'_1 and F'_2, are further cut-up into sub-carriers of UL and DL denoted respectively as $F'_2 = F'_{2,UL} + F'_{2,DL}$ and $F'_1 = F'_{1,UL} + F'_{1,DL}$ for notation clarity.

3 Coverage probability

This section focus on the assessment of coverage probability in the proposed network scenarios where v is assumed to be located in A_2 and in A_1; (i) uplink coverage probability for uniform HetNets (UHs') is presented in Subsection 3.1 while (ii) the uplink coverage probability in case of non-uniform HetNets (NUHs') is derived in Subsection 3.2.

3.1 Uplink coverage probability for uniform HetNets (UHs)

The UL coverage probability when there are intentional jammers (IJs) and RFA, $P^{UL,*}_{A_2}(\Gamma_M)$, while considering v in A_2 can be obtained as:

$$P^{UL,*}_{A_2}(\Gamma_M) = P\left(SIR^{UL}_M > \Gamma_M\right). \tag{1}$$

Following the architecture of RFA, the total interference in UL is the addition of the UL interference from MBSs in A_2, i.e., $I^{UL}_{\phi_M,A_2}$, the DL interference from SBSs in A_1, i.e., $I^{DL}_{\phi_s,A_1}$, and the interference from IJs, i.e., $I_{J,A}$. Therefore, SIR^{UL}_M from (1) can be written as:

$$SIR^{UL}_M = \frac{P^{UL}_{t,v}|h_M|^2 r_M^{-\alpha}}{I^{UL}_{\phi_M,A_2} + I^{DL}_{\phi_S,A_1} + I_{\phi_J,A}}. \tag{2}$$

Eq (2) can be expanded as:

$$SIR^{UL}_M = \frac{P^{UL}_{t,v}|h_M|^2 r_M^{-\alpha}}{\sum_{l\in\phi_M} P^{UL}_{t,l}|h_l|^2 r_l^{-\alpha} + \sum_{k\in\phi_S} P^{DL}_{t,k}|h_k|^2 r_k^{-\alpha} + \sum_{j\in\phi_J} P_{t,j}|h_j|^2 r_j^{-\alpha}}. \tag{3}$$

In (3), $P^{UL}_{t,l}$ is the v UL transmission power connected with MBS, $P^{DL}_{t,k}$ is the transmission power of SBS, and $P_{t,j}$ is the emitting power of jammers. Moreover, substituting (2) into (1), we obtain $P^{UL,*}_{A_2}(\Gamma_M)$ as:

$$\begin{aligned} P^{UL,*}_{A_2}(\Gamma_M) &\overset{(1)}{=} P\left(\frac{P^{UL}_{t,v}|h_M|^2 r_M^{-\alpha}}{I^{UL}_{\phi_M,A_2} + I^{DL}_{\phi_S,A_1} + I_{\phi_J,A}} > \Gamma_M\right) \\ &\overset{(2)}{=} E_{r_M, I^{UL}_{\phi_M,A_2}, I^{DL}_{\phi_S,A_1}, I_{\phi_J,A}}\left[\exp\left(-\frac{r_M^{\alpha}\Gamma_M}{P^{UL}_{t,v}}\left(I^{UL}_{\phi_M,A_2} + I^{DL}_{\phi_S,A_1} + I_{\phi_J,A}\right)\right)\right] \\ &\overset{(3)}{=} E_{r_M}\left[\mathcal{L}_{I^{UL}_{\phi_M,A_2}}(s) \times \mathcal{L}_{I^{DL}_{\phi_S,A_1}}(s) \times \mathcal{L}_{I_{\phi_J,A}}(s)\right]\Big|_{s=\frac{r_M^{\alpha}\Gamma_M}{P^{UL}_{t,v}}}. \end{aligned} \tag{4}$$

Here, Step (1) follows from the coverage probability definition [17, 40]. Step (2) follows from Step (1) by using the void property of IHPPPs [40]. Similarly, Step (3) is obtained by replacing $\frac{r_M^{\alpha}\Gamma_M}{P^{UL}_{t,v}}$ by s, where $s = \frac{r_M^{\alpha}\Gamma_M}{P^{UL}_{t,v}}$. In addition, Stage (4) is obtained by the use of the exponential property of additions in products i.e., $\exp(a + b) = \exp(a) \times \exp(b)$.

The Laplace transform (LT) of interference in UL from MBSs in A_2, i.e., $\mathcal{L}_{I^{\mathrm{UL}}_{\phi_{\mathrm{M}},A_2}}$, is obtained as:

$$\begin{aligned}
\mathcal{L}_{I^{\mathrm{UL}}_{\phi_{\mathrm{M}},A_2}}(s) &\overset{(a)}{=} \mathrm{E}_{I^{\mathrm{UL}}_{\phi_{\mathrm{M}},A_2}}\left[\exp\left(-I^{\mathrm{UL}}_{\phi_{\mathrm{M}},A_2}s\right)\right]\Big|_{s=\frac{r_{\mathrm{M}}^{\alpha}\Gamma_{\mathrm{M}}}{P^{\mathrm{UL}}_{t,v}}} \\
&\overset{(b)}{=} \mathrm{E}_{I^{\mathrm{UL}}_{\phi_{\mathrm{M}},A_2},|h_l|^2}\left[\exp\left(-s\sum_{l\in\phi_{\mathrm{M}}}P^{\mathrm{UL}}_{t,v}|h_l|^2 r_l^{-\alpha}\right)\right] \\
&\overset{(c)}{=} \mathrm{E}_{I^{\mathrm{UL}}_{\phi_{\mathrm{M}},A_2},|h_l|^2}\left[\prod_{l\in\phi_{\mathrm{M}}}\exp\left(-|h_l|^2\Gamma_{\mathrm{M}}r_{\mathrm{M}}^{\alpha}r_l^{-\alpha}\right)\right] \\
&\overset{(d)}{=} \mathrm{E}_{I^{\mathrm{UL}}_{\phi_{\mathrm{M}},A_2}}\left[\prod_{l\in\phi_{\mathrm{M}}}\mathrm{E}_{|h_l|^2}\exp\left(-|h_l|^2\Gamma_{\mathrm{M}}r_{\mathrm{M}}^{\alpha}r_l^{-\alpha}\right)\right] \\
&\overset{(e)}{=} \mathrm{E}_{I^{\mathrm{UL}}_{\phi_{\mathrm{M}},A_2}}\left[\prod_{l\in\phi_{\mathrm{M}}}\frac{1}{1+\Gamma_{\mathrm{M}}\left(\frac{r_l}{r_{\mathrm{M}}}\right)^{-\alpha}}\right] \\
&\overset{(f)}{=} \exp\left(-2\pi\zeta_{\mathrm{M}}\int_{\Delta s_1}^{\Delta s_2}\frac{r_l dr_l}{1+\left(\frac{r_l}{\Gamma_{\mathrm{M}}^{1/\alpha}r_{\mathrm{M}}}\right)^{\alpha}}\right) \\
&\overset{(g)}{=} \exp\left(-\pi\zeta_{\mathrm{M}}\Gamma_{\mathrm{M}}^{2/\alpha}r_{\mathrm{M}}^2\int_{\left(\frac{\Delta s_1}{\Gamma_{\mathrm{M}}^{1/\alpha}r_{\mathrm{M}}}\right)^2}^{\left(\frac{\Delta s_2}{\Gamma_{\mathrm{M}}^{1/\alpha}r_{\mathrm{M}}}\right)^2}\frac{du}{1+(u)^{\alpha/2}}\right) \\
&\overset{(h)}{=} \exp\left(\frac{\zeta_{\mathrm{M}}\pi\Gamma_{\mathrm{M}}\Delta s_2^{(2-\alpha)}r_{\mathrm{M}}^{\alpha}}{\alpha/2-1}{}_2F_1\left(1,1-\frac{2}{\alpha},2-\frac{2}{\alpha},-\Gamma_{\mathrm{M}}\left(\frac{r_{\mathrm{M}}}{\Delta s_2}\right)^{\alpha}\right)-\right. \\
&\left.\frac{\zeta_{\mathrm{M}}\pi\Gamma_{\mathrm{M}}\Delta s_1^{(2-\alpha)}r_{\mathrm{M}}^{\alpha}}{\alpha/2-1}{}_2F_1\left(1,1-\frac{2}{\alpha},2-\frac{2}{\alpha},-\Gamma_{\mathrm{M}}\left(\frac{r_{\mathrm{M}}}{\Delta s_1}\right)^{\alpha}\right)\right).
\end{aligned} \tag{5}$$

Here, Step (*a*) follows the definition of LT [40], Step (*b*) is achieved by substituting $I^{\mathrm{UL}}_{\phi_{\mathrm{M}},A_2}=\sum_{l\in\phi_{\mathrm{M}}}P^{\mathrm{UL}}_{t,l}|h_l|r_l^{-\alpha}$, into Step (*a*), Step (*c*) is achieved by replacing *s*, s.t., $s=\frac{r_{\mathrm{M}}^{\alpha}\Gamma_{\mathrm{M}}}{P^{\mathrm{UL}}_{t,v}}$, into Step (*b*), Step (*e*) is followed by evaluating the LT of Step (*d*) with respect to h_j, Step (*f*), is followed by considering probability generating functional (PGFL) of IHPPP [47], Step (*g*) is achieved by replacing $u=\left(\frac{r_j}{(\Gamma_{\mathrm{M}})^{1/\alpha}r_{\mathrm{M}}}\right)^2$ into Step (*f*), and Step (*h*) is achieved from Gauss-hypergeometric approximation of Step (*g*) [47].

Similarly, the LT of the total UL interference received from the MBSs in A_1, i.e., $\mathcal{L}_{I^{\mathrm{UL}}_{\phi_{\mathrm{M}},A_1}}(s)$, is obtained as:

$$\begin{aligned}&\mathcal{L}_{I^{\mathrm{UL}}_{\phi_{\mathrm{M}},A_2}}(s)\\&=\exp\left(\frac{\zeta_{\mathrm{M}}\pi\Gamma_{\mathrm{M}}\Delta s_2^{(2-\alpha)}r_{\mathrm{M}}^{\alpha}}{\alpha/2-1}{}_2F_1\left(1,1-\frac{2}{\alpha},2-\frac{2}{\alpha},-\Gamma_{\mathrm{M}}\left(\frac{r_{\mathrm{M}}}{\Delta s_2}\right)^{\alpha}\right)\right.\\&\left.-\frac{\zeta_{\mathrm{M}}\pi\Gamma_{\mathrm{M}}\Delta s_1^{(2-\alpha)}r_{\mathrm{M}}^{\alpha}}{\alpha/2-1}{}_2F_1\left(1,1-\frac{2}{\alpha},2-\frac{2}{\alpha},-\Gamma_{\mathrm{M}}\left(\frac{r_{\mathrm{M}}}{\Delta s_1}\right)^{\alpha}\right)\right).\end{aligned}\tag{6}$$

In addition, the LT of the DL interference from SBSs in A_1, i.e., $\mathcal{L}_{I^{\mathrm{DL}}_{\phi_{\mathrm{S}},A_1}}$, can be written in a similar way as far (5), and is given as:

$$\begin{aligned}&\mathcal{L}_{I^{\mathrm{DL}}_{\phi_{\mathrm{S}},A_1}}=\\&\exp\left(\frac{\zeta_{\mathrm{S}}'\pi\eta_3\Gamma_{\mathrm{M}}x_2^{(2-\alpha)}r_{\mathrm{M}}^{\alpha}}{\alpha/2-1}{}_2F_1\left(1,1-\frac{2}{\alpha},2-\frac{2}{\alpha},-\eta_3\Gamma_{\mathrm{M}}\left(\frac{r_{\mathrm{M}}}{x_2}\right)^{\alpha}\right)-\right.\\&\left.\frac{\zeta_{\mathrm{S}}'\pi\eta_3\Gamma_{\mathrm{M}}x_1^{(2-\alpha)}r_{\mathrm{M}}^{\alpha}}{\alpha/2-1}{}_2F_1\left(1,1-\frac{2}{\alpha},2-\frac{2}{\alpha},-\eta_3\Gamma_{\mathrm{M}}\left(\frac{r_{\mathrm{M}}}{x_1}\right)^{\alpha}\right)\right).\end{aligned}\tag{7}$$

$$\begin{aligned}&\mathcal{L}_{I_{\phi_J,A}}(s)=\\&\exp\left(\frac{\zeta_j\pi\eta_2\Gamma_{\mathrm{M}}z_2^{(2-\alpha)}r_{\mathrm{M}}^{\alpha}}{\alpha/2-1}{}_2F_1\left(1,1-\frac{2}{\alpha},2-\frac{2}{\alpha},-\eta_2\Gamma_{\mathrm{M}}\left(\frac{r_{\mathrm{M}}}{z_2}\right)^{\alpha}\right)-\right.\\&\left.\frac{\zeta_j\pi\eta_2\Gamma_{\mathrm{M}}z_1^{(2-\alpha)}r_{\mathrm{M}}^{\alpha}}{\alpha/2-1}{}_2F_1\left(1,1-\frac{2}{\alpha},2-\frac{2}{\alpha},-\eta_2\Gamma_{\mathrm{M}}\left(\frac{r_{\mathrm{M}}}{z_1}\right)^{\alpha}\right)\right).\end{aligned}\tag{8}$$

η_2 is the ratio of $P_{t,S}^{\mathrm{DL}}$ and $P_{t,v}^{\mathrm{UL}}$ where $P_{t,S}^{\mathrm{DL}}$ is the DL transmit power of SBSs.

The UL coverage probability, $P_{A_2}^{\mathrm{UL},*}(\Gamma_{\mathrm{M}})$, in the presence of ICI, IJI, and RFA employment while considering v in A_2 can be written as [17]

$$\begin{aligned}&P_{A_2}^{\mathrm{UL},*}(\Gamma_{\mathrm{M}})=\int_{\Delta s_1}^{d_2}\mathcal{L}_{I^{\mathrm{UL}}_{\phi_{\mathrm{M}},A_2}}(s)\times\mathcal{L}_{I^{\mathrm{DL}}_{\phi_{\mathrm{S}},A_1}}(s)\times\mathcal{L}_{I_{\phi_J,A}}(s)\\&f_{r_{\mathrm{M},v}|v_{A_2}}(r_{\mathrm{M},v})dr_{\mathrm{M},v}.\end{aligned}\tag{9}$$

$$\begin{aligned}P_{A_2}^{\mathrm{UL},*}(\Gamma_{\mathrm{M}})=\frac{2\pi\zeta_{\mathrm{M}}}{\exp(-\zeta_{\mathrm{M}}\pi d_1^2)}\int_{\Delta s_1}^{\Delta s_2}\exp\left(\frac{\pi\Gamma_{\mathrm{M}}r_{\mathrm{M}}^{\alpha}}{\alpha/2-1}\left[\zeta_{\mathrm{M}}\Delta s_2^{(2-\alpha)}\mathcal{J}\left(\alpha,-\Gamma_{\mathrm{M}}\left(\frac{r_{\mathrm{M}}}{\Delta s_2}\right)^{\alpha}\right)-\zeta_{\mathrm{M}}\Delta s_1{}^{(2-\alpha)}\mathcal{J}\left(\alpha,-\Gamma_{\mathrm{M}}\left(\frac{r_{\mathrm{M}}}{\Delta s_1}\right)^{\alpha}\right).\right.\right.\\+\zeta_{\mathrm{S}}'\eta_3\Delta s_1^{(2-\alpha)}\mathcal{J}\left(\alpha,-\Gamma_{\mathrm{M}}\eta_3\left(\frac{r_{\mathrm{M}}}{\Delta s_1}\right)^{\alpha}\right)-\zeta_{\mathrm{S}}'\eta_3 y^{(2-\alpha)}\mathcal{J}\left(\alpha,-\Gamma_{\mathrm{M}}\eta_3\left(\frac{r_{\mathrm{M}}}{y}\right)^{\alpha}\right)+\zeta_j\eta_2\Delta s_2^{(2-\alpha)}\mathcal{J}\left(\alpha,-\Gamma_{\mathrm{M}}\eta_2\left(\frac{r_{\mathrm{M}}}{\Delta s_2}\right)^{\alpha}\right)\\\left.\left.-\zeta_j\eta_2 y^{(2-\alpha)}\mathcal{J}\left(\alpha,-\Gamma_{\mathrm{M}}\eta_2\left(\frac{r_{\mathrm{M}}}{y}\right)^{\alpha}\right)\right]-\zeta_{\mathrm{M}}\pi r_{\mathrm{M}}^2\right)r_{\mathrm{M}}dr_{\mathrm{M}}.\end{aligned}\tag{10}$$

$$P_{A_2}^{\mathrm{UL}}(\Gamma_{\mathrm{M}}) = \frac{2\pi\zeta_{\mathrm{M}}}{\exp(-\zeta_{\mathrm{M}}\pi d_1^2)} \int_{\Delta s_1}^{\Delta s_2} \exp\left(\frac{\pi\Gamma_{\mathrm{M}} r_{\mathrm{M}}^{\alpha}}{\alpha/2-1} \left[\zeta_{\mathrm{M}} \Delta s_2^{(2-\alpha)} \mathcal{J}\left(\alpha, -\Gamma_{\mathrm{M}}\left(\frac{r_{\mathrm{M}}}{\Delta s_2}\right)^{\alpha}\right) - \zeta_{\mathrm{M}} \Delta s_1{}^{(2-\alpha)} \mathcal{J}\left(\alpha, -\Gamma_{\mathrm{M}}\left(\frac{r_{\mathrm{M}}}{\Delta s_1}\right)^{\alpha}\right) \right.\right.$$
$$\left.\left. + \zeta_j \eta_2 \Delta s_2^{(2-\alpha)} \mathcal{J}\left(\alpha, -\Gamma_{\mathrm{M}}\eta_2\left(\frac{r_{\mathrm{M}}}{\Delta s_2}\right)^{\alpha}\right) - \zeta_j \eta_2 y^{(2-\alpha)} \mathcal{J}\left(\alpha, -\Gamma_{\mathrm{M}}\eta_2\left(\frac{r_{\mathrm{M}}}{y}\right)^{\alpha}\right) \right] - \zeta_{\mathrm{M}}\pi r_{\mathrm{M}}^2 \right) r_{\mathrm{M}} dr_{\mathrm{M}}. \quad (11)$$

By substituting (6), (7), and (8) into (9), $P_{A_2}^{\mathrm{UL},*}(\Gamma_{\mathrm{M}})$ is expressed as (10).

3.2 Uplink coverage probability for non-uniform HetNets (NUHs')

Non-uniform heterogeneous network deployment is established where SBS in A_1 is muted and user in that vicinity is in coverage with MBS. The UL coverage probability, $P_{A_2}^{\mathrm{UL}}(\Gamma_{\mathrm{M}})$, while assuming IJs, RFA, and v in A_2 can be written as

$$P_{A_2}^{\mathrm{UL}}(\Gamma_{\mathrm{M}}) = \int_{\Delta s_1}^{d_2} \mathcal{L}_{I_{\phi_{\mathrm{M}},A_2}^{\mathrm{UL}}}(s) \times \mathcal{L}_{I_{\phi_J,A}}(s) f_{r_{\mathrm{M},v}|v_{A_2}}(r_{\mathrm{M},v}) dr_{\mathrm{M},v}. \quad (12)$$

By substituting (6) and (8) into (12), $P_{A_1}^{\mathrm{UL}}(\Gamma_{\mathrm{M}})$ is expressed as (11). In (10) and (11), $\mathcal{J}(\cdot)$ indicates the Gauss-hypergeometric function.

4 Results and discussion

This section describes results for the user's UL coverage probability while taking into consideration: (i) UL coverage probability of UH and (ii) UL coverage probability of NUH. MATLAB 2015a has been used in drawing our results. MBS, SBS, jammers and users are dispersed in $A = \pi(500\mathrm{m})^2$, s.t., $A = A_1 \mathrm{U} A_2$. Transmitted power by MBS, SBS, jammers, and users are supposed to be 40 dBm, 30 dBm, 20 dBm, and 20 dBm, respectively. Various network parameters such as ζ_{M}, ζ_{S}, ζ_j, Γ_{M}, $P_{t,J}$ and $P_{t,u}^{\mathrm{UL}}$ are assumed for analyzing UL coverage when the user is located in A_2.

Fig 3 compares UL coverage probability for different values of Γ_{M} in A_2. This figure assumes $\zeta_j = 0$ and 100, for both UH and NUH network scenarios. This figure indicates that the simulation results will coincide with the numerical results both for UH and NUH. The plots in the figure further demonstrate that NUHs with $\zeta_j = 0$ lead to the highest coverage gain as compared with the rest of the scenarios. This is due to improved interference mitigation by NUHs as a result of lower SBS deployment.

In Fig 4, we demonstrate UL coverage probability against different values of Γ_{M} for both UH and NUH in A_2. This figure is obtained for $\zeta_j = 0$ and 100 and $\zeta_{\mathrm{S}}/\zeta_{\mathrm{M}} = 30$. This result demonstrates that NUH with RFA outperforms the other scenarios due to significant interference mitigation. At $\Gamma_{\mathrm{M}} = -10dB$, the proposed NUH with RFA and $\zeta_j = 0$ leads to 20% UL coverage gain.

In Fig 5A and 5B, we compare UL coverage probability against different values of Γ_{M} for UH and NUH, respectively. The plots in both the figures are obtained for $\zeta_j = 0$, 100, 200, 300, 400, 500. Moreover, the results indicate that a sufficient number of IJs in the network are needed to significantly degrade UL coverage because of the wideband nature and low transmission power of IJs. Furthermore, increasing the value ζ_j leads to lower UL coverage in both UH and NUH due to higher interference. The results indicate significant coverage performance improvements by RFA and NUH due to effective interference mitigation.

In Fig 6A and 6B, we evaluate UL coverage probability for different values of ζ_j, while considering RFA, UH, and NUH. The plots are obtained for $\Gamma_{\mathrm{M}} = 0$ dB, −5 dB, −10 dB, −15 dB,

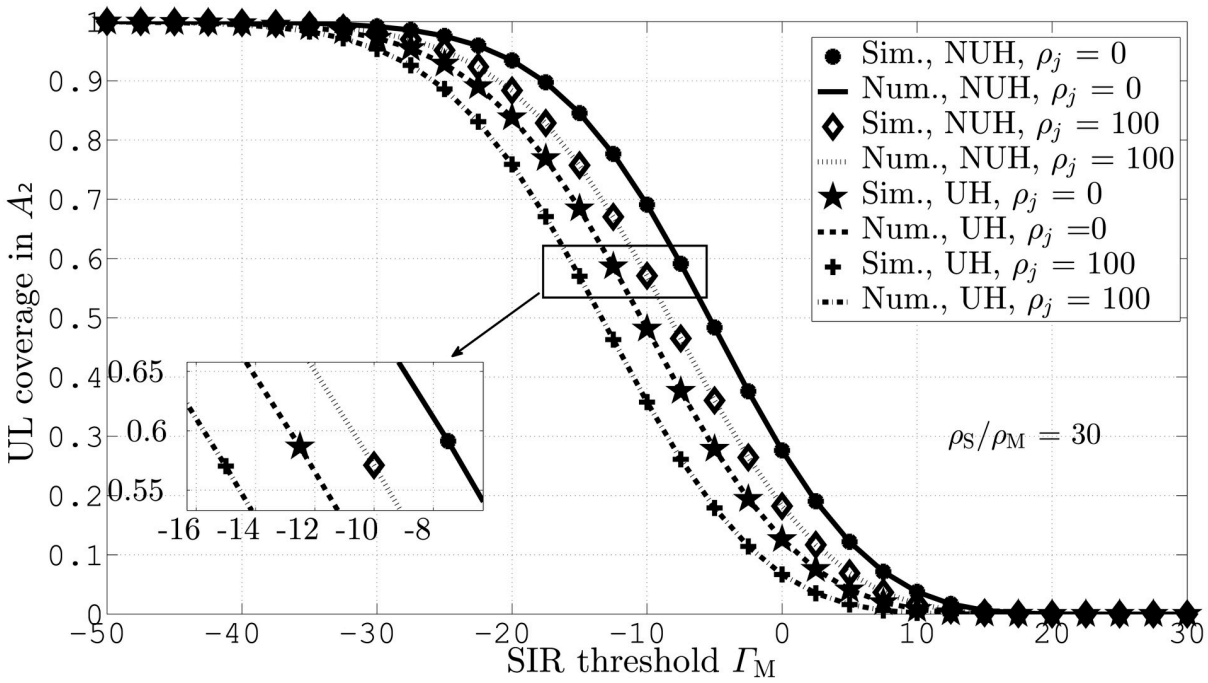

Fig 3. UL coverage probabilities against Γ_M and ζ_j in A_2.

https://doi.org/10.1371/journal.pone.0287709.g003

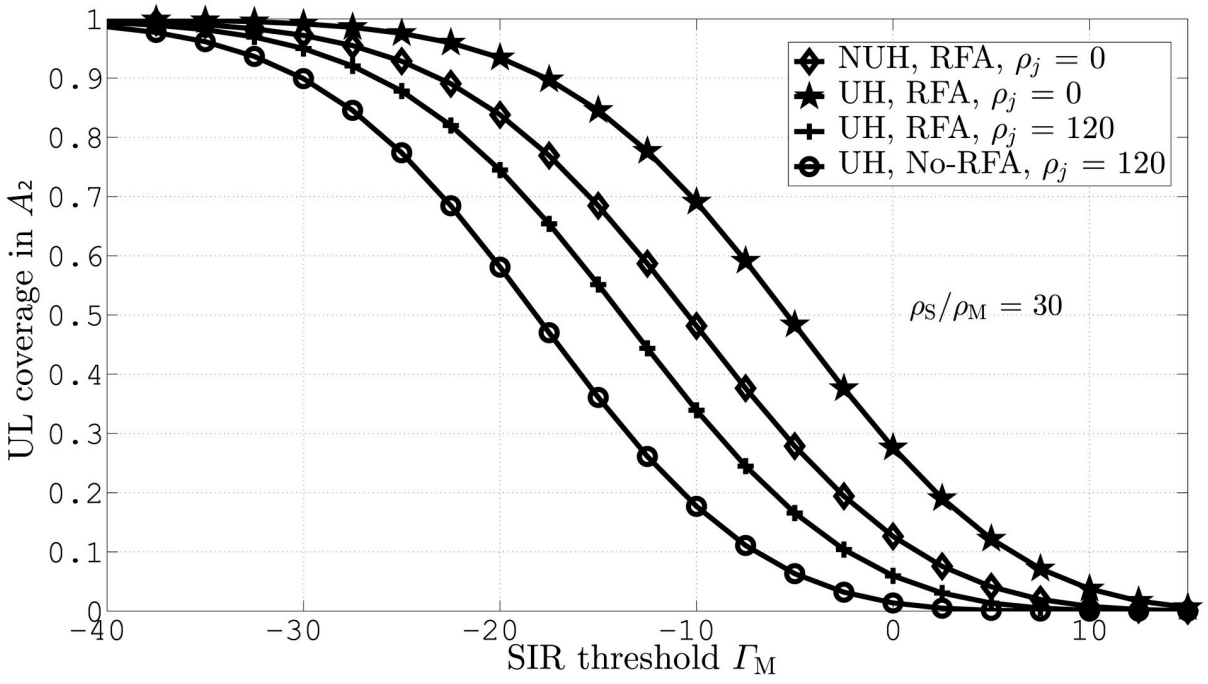

Fig 4. UL coverage probabilities for UH and NUH in A_2.

https://doi.org/10.1371/journal.pone.0287709.g004

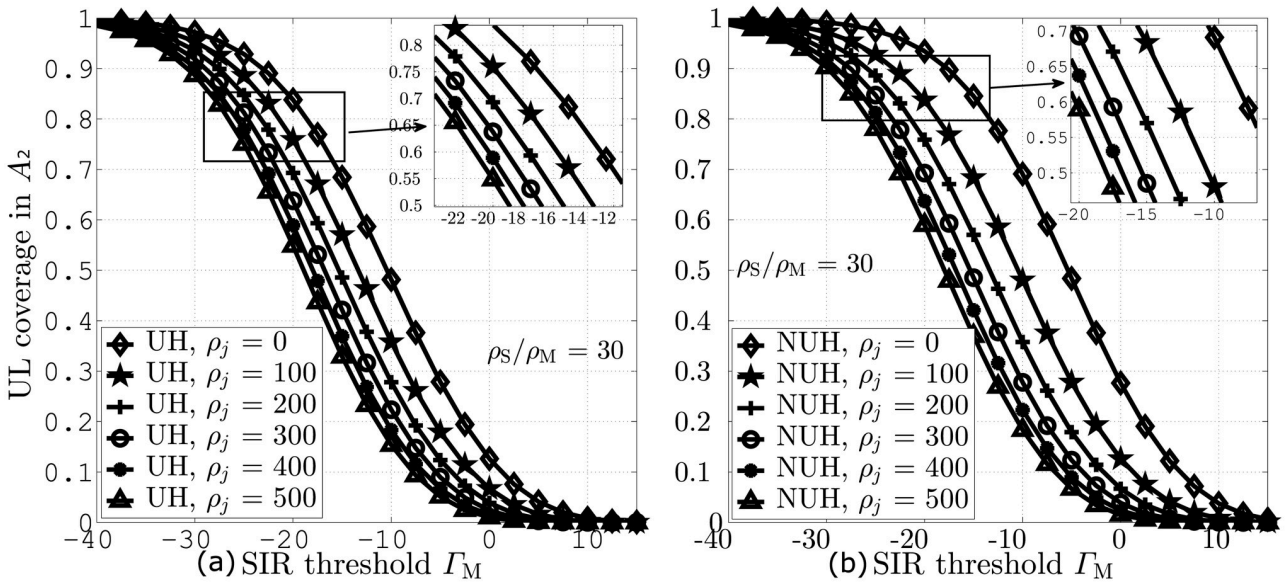

Fig 5. UL coverage probabilities against Γ_M and ζ_j. A: UH B: NUH.

https://doi.org/10.1371/journal.pone.0287709.g005

−20 dB, −25 dB and $\zeta_S/\zeta_M = 30$. The plots indicate that higher values of Γ_M lead to lower coverage due to lower user association. Furthermore, the plots in both figures indicate that NUH gives rise to higher coverage in contrast to UH. By employing RFA, the network performance improves in both cases but due to less interference the coverage in NUH is better than UH.

Similarly, Fig 7A and 7B demonstrate UL coverage performance against IJs distribution area for different values of ζ_j and $\zeta_S/\zeta_M = 10$.

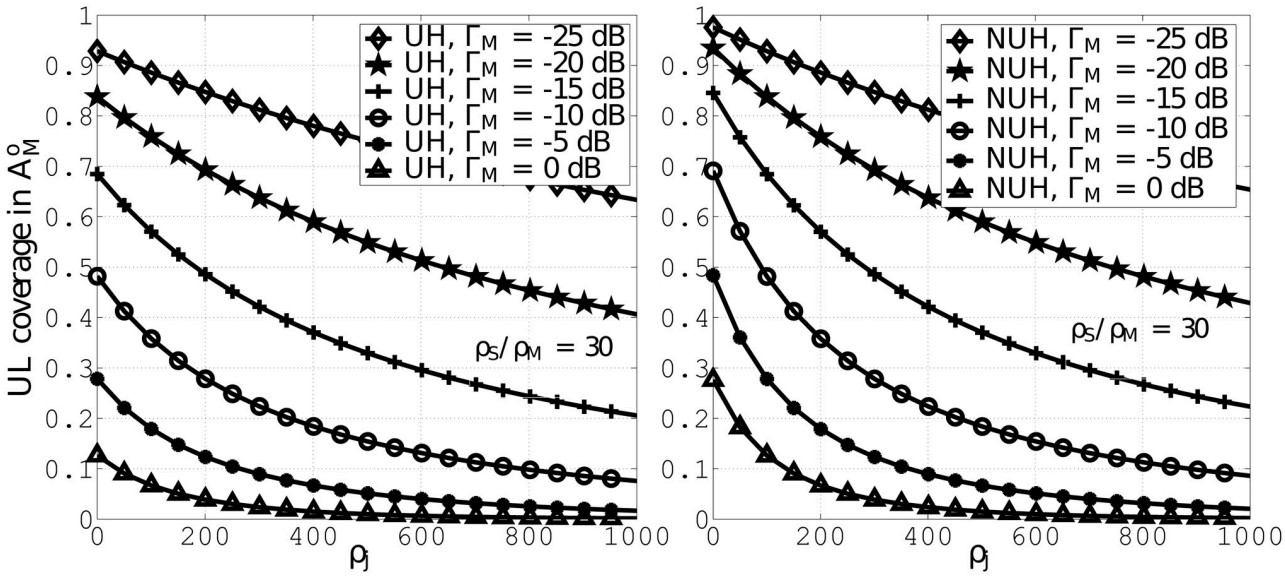

Fig 6. UL coverage probabilities against ζ_j. A: UH B: NUH.

https://doi.org/10.1371/journal.pone.0287709.g006

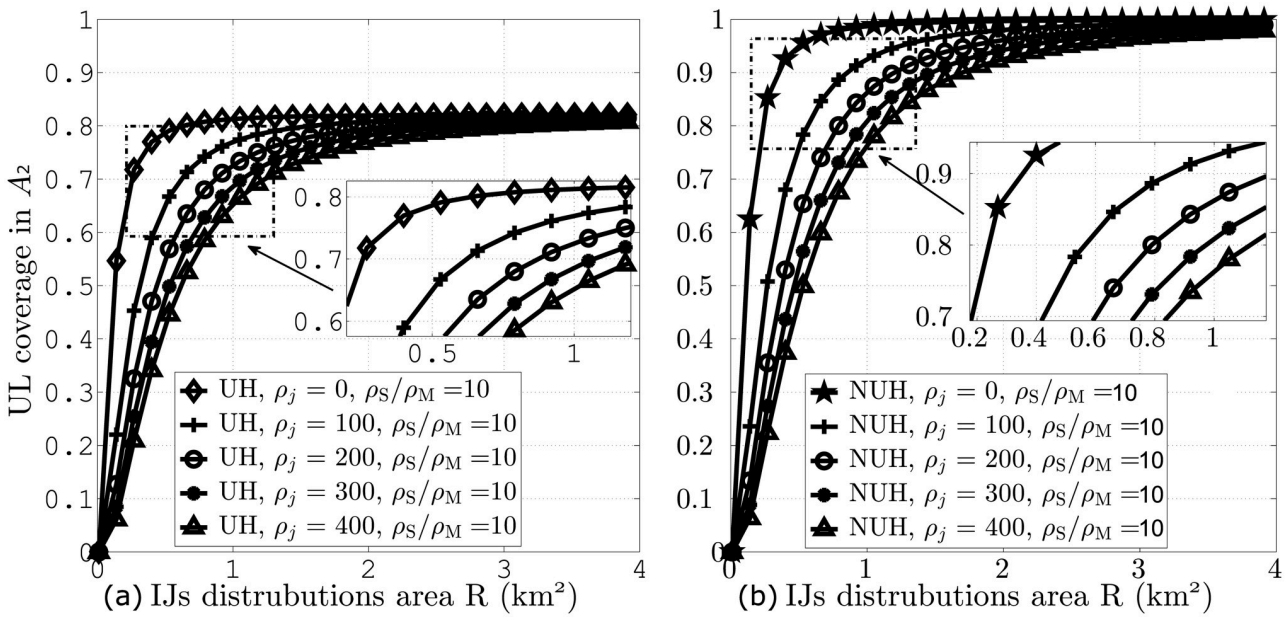

Fig 7. UL coverage probabilities against IJs distribution area for different values of ζ_j and ζ_S/ζ_M = 10. A: UH B: NUH.

https://doi.org/10.1371/journal.pone.0287709.g007

Both of these figures indicate that increasing IJs distribution area leads to improved coverage as the IJs become less effective. The figures further depict that at an area of 1 km^2, NUH with RFA leads to 19% UL coverage improvement due to significant interference reduction.

Finally, Fig 8A and 8B show UL coverage probability against IJs distribution area for different values of Γ_M. These figures consider ζ_j = 100 and ζ_S/ζ_M = 10. The results indicate that increase in the values of Γ_M gives rise to lower coverage due to lower user connection. The

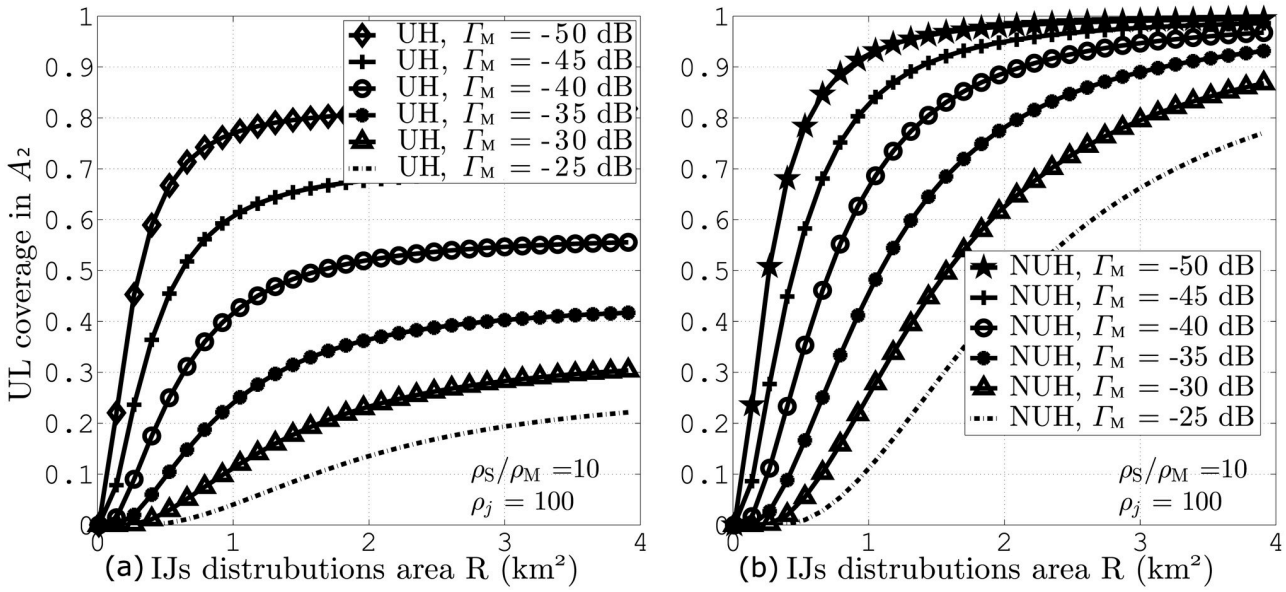

Fig 8. UL coverage probabilities against IJs distribution area for different values of Γ_M and ζ_j = 100. A: UH B: NUH.

https://doi.org/10.1371/journal.pone.0287709.g008

figures also indicate that NUH with RFA and Γ_M = -50 dB give rise to the highest coverage gain in contrast to the rest of the scenarios.

5 Conclusion

This work aims to reduce ICI and IJI by employing SBS muting and RFA in HetNets. Various network parameters such as jammer's density, jammers transmit power and their distribution area, SIR threshold are investigated against user coverage. The results are obtained for both UHs and NUHs in addition to and without RFA. The results depict that NUHs employing RFA outperform other scenarios in terms of UL coverage. Moreover, the investigation indicates 20% UL coverage improvement at $\Gamma_M = -10$ dB while using RFA and NUHs as compared with RFA and UHs. This work can be extended to evaluate drone-based jammers in HetNets.

Author Contributions

Conceptualization: Saleh Mohammed Ghonaim, Samar Khan, Muhammad Sajid Haroon.

Data curation: Samar Khan, Muhammad Irfan.

Formal analysis: Saleh Mohammed Ghonaim, Samar Khan, Faisal Althobiani, Muhammad Irfan.

Funding acquisition: Faisal Althobiani, Shadi Alghaffari, Fazal Muhammad.

Investigation: Saleh Mohammed Ghonaim, Sheraz Khan, Fazal Muhammad.

Methodology: Faisal Althobiani.

Project administration: Sheraz Khan, Muhammad Irfan, Muhammad Sajid Haroon.

Resources: Shadi Alghaffari, Sheraz Khan, Muhammad Irfan, Muhammad Sajid Haroon, Fazal Muhammad.

Software: Muhammad Sajid Haroon.

Supervision: Faisal Althobiani, Shadi Alghaffari, Sheraz Khan, Muhammad Irfan, Muhammad Sajid Haroon, Fazal Muhammad.

Validation: Saleh Mohammed Ghonaim, Samar Khan, Shadi Alghaffari, Sheraz Khan.

Visualization: Faisal Althobiani.

Writing – original draft: Saleh Mohammed Ghonaim, Samar Khan.

Writing – review & editing: Faisal Althobiani, Shadi Alghaffari, Sheraz Khan, Muhammad Irfan, Muhammad Sajid Haroon, Fazal Muhammad.

References

1. Ghosh SK, Ghosh SC. Performance analysis of dual connectivity in control/user-plane split heterogeneous networks. Computer Communications. 2020 Jan 1; 149:370–81. https://doi.org/10.1016/j.comcom.2019.10.032
2. Fadoul MM. Rate and coverage analysis in multi-tier heterogeneous network using stochastic geometry approach. Ad Hoc Networks. 2020 Mar 1; 98:102038. https://doi.org/10.1016/j.adhoc.2019.102038
3. Olfat E, Bengtsson M. A general framework for joint estimation-detection of channel, nonlinearity parameters and symbols for OFDM in IoT-based 5G networks. Signal Processing. 2020 Feb 1; 167:107298. https://doi.org/10.1016/j.sigpro.2019.107298
4. Bogale TE, Le LB. Massive MIMO and millimeter wave for 5G wireless HetNet: potentials and challenges. arXiv preprint arXiv:1510.06359. 2015 Oct 21.

5. Ouali K, Kassar M, Nguyen TM, Sethom K, Kervella B. An efficient D2D handover management scheme for SDN-based 5G networks. In 2020 IEEE 17th Annual Consumer Communications & Networking Conference (CCNC) 2020 Jan 10 (pp. 1–6). IEEE.
6. Qamar F, Hindia MN, Dimyati K, Noordin KA, Amiri IS. Interference management issues for the future 5G network: a review. Telecommunication Systems. 2019 Aug 15; 71:627–43. https://doi.org/10.1007/s11235-019-00578-4
7. Ramazanali H, Mesodiakaki A, Vinel A, Verikoukis C. Survey of user association in 5G HetNets. In 2016 8th IEEE Latin-American conference on communications (LATINCOM) 2016 Nov 15 (pp. 1–6). IEEE.
8. Sada AS, Abdullahi ZM, Usman AD, Tekanyi AM, Mubarak AU, Maiwada YA. Modified Handover Decision Algorithm in Long Term Evolution Advanced Network. In 2019 2nd International Conference of the IEEE Nigeria Computer Chapter (NigeriaComputConf) 2019 Oct 14 (pp. 1–4). IEEE.
9. Dao NN, Park M, Kim J, Paek J, Cho S. Resource-aware relay selection for inter-cell interference avoidance in 5G heterogeneous network for Internet of Things systems. Future Generation Computer Systems. 2019 Apr 1; 93:877–87. https://doi.org/10.1016/j.future.2018.03.037
10. Xu J, Lee SJ, Kang WS, Seo JS. Adaptive resource allocation for MIMO-OFDM based wireless multicast systems. IEEE Transactions on Broadcasting. 2010 Feb 5; 56(1):98–102. https://doi.org/10.1109/TBC.2009.2039691
11. IJEMARU GK, OLEKA EU, NGHARAMIKE ET, Njokuocha KI, UDUNWA AI. Inter-Cell Interference Mitigation Techniques in a Heterogeneous LTE-Advanced Access Network.
12. Tsiota A, Xenakis D, Passas N, Merakos L. On jamming and black hole attacks in heterogeneous wireless networks. IEEE Transactions on Vehicular Technology. 2019 Aug 29; 68(11):10761–74. https://doi.org/10.1109/TVT.2019.2938405
13. Arjoune Y, Faruque S. Smart jamming attacks in 5G new radio: A review. In2020 10th annual computing and communication workshop and conference (CCWC) 2020 Jan 6 (pp. 1010–1015). IEEE.
14. Tian P, Tian H, Zhu J, Chen L, She X. An adaptive bias configuration strategy for range extension in LTE-advanced heterogeneous networks. InIET international conference on communication technology and application (ICCTA 2011) 2011 Oct 14 (pp. 336–340). IET.
15. Muhammad F, Haroon MS, Abbas ZH, Abbas G, Kim S. Uplink interference management for HetNets stressed by clustered wide-band jammers. IEEE access. 2019 Dec 17; 7:182679–90. https://doi.org/10.1109/ACCESS.2019.2960278
16. Wu H, Wei Z, Hou Y, Zhang N, Tao X. Cell-edge user offloading via flying UAV in non-uniform heterogeneous cellular networks. IEEE Transactions on Wireless Communications. 2020 Jan 14; 19(4):2411–26. https://doi.org/10.1109/TWC.2020.2964656
17. Haroon MS, Abbas ZH, Muhammad F, Abbas G. Analysis of coverage-oriented small base station deployment in heterogeneous cellular networks. Physical Communication. 2020 Feb 1; 38:100908. https://doi.org/10.1016/j.phycom.2019.100908
18. Haroon MS, Abbas ZH, Muhammad F, Abbas G. Coverage analysis of cell-edge users in heterogeneous wireless networks using Stienen's model and RFA scheme. International Journal of Communication Systems. 2020 Jul 10; 33(10):e4147. https://doi.org/10.1002/dac.4147
19. Kuribayashi HP, De Souza MA, Gomes DD, Silva KD, Da Silva MS, Costa JC, et al. Particle swarm-based cell range expansion for heterogeneous mobile networks. IEEE Access. 2020 Feb 24; 8:37021–34. https://doi.org/10.1109/ACCESS.2020.2975981
20. Novlan TD, Ganti RK, Ghosh A, Andrews JG. Analytical evaluation of fractional frequency reuse for heterogeneous cellular networks. IEEE Transactions on Communications. 2012 Jun 18; 60(7):2029–39. https://doi.org/10.1109/TCOMM.2012.061112.110477
21. Ijaz A, Hassan SA, Zaidi SA, Jayakody DN, Zaidi SM. Coverage and rate analysis for downlink HetNets using modified reverse frequency allocation scheme. IEEE access. 2017 Feb 17; 5:2489–502. https://doi.org/10.1109/ACCESS.2017.2670027
22. Chih-Lin I, Han S, Xu Z, Sun Q, Pan Z. 5G: rethink mobile communications for 2020+. Philosophical Transactions of the Royal Society A: Mathematical, Physical and Engineering Sciences. 2016 Mar 6; 374(2062):20140432. https://doi.org/10.1098/rsta.2014.0432 PMID: 26809577
23. Bogale TE, Le LB. Massive MIMO and mmWave for 5G wireless HetNet: Potential benefits and challenges. IEEE Vehicular Technology Magazine. 2016 Feb 3; 11(1):64–75. https://doi.org/10.1109/MVT.2015.2496240
24. Swami P, Bhatia V, Vuppala S, Ratnarajah T. User fairness in NOMA-HetNet using optimized power allocation and time slotting. IEEE Systems Journal. 2020 Mar 9; 15(1):1005–14. https://doi.org/10.1109/JSYST.2020.2975250
25. Liu W, Tian L, Sun JX. Interference alignment for MIMO downlink heterogeneous networks. IEEE Access. 2020 Feb 17; 8:35090–104. https://doi.org/10.1109/ACCESS.2020.2974584

26. Chaieb C, Mlika Z, Abdelkefi F, Ajib W. On the optimization of user association and resource allocation in HetNets with mm-wave base stations. IEEE Systems Journal. 2020 Jun 16; 14(3):3957–67. https://doi.org/10.1109/JSYST.2020.2984596

27. Jazea NA, Kadim HA, Sallomi AH. Study and analysis of intra-cell interference and inter-cell interference for 5G network. Journal of Engineering and Sustainable Development. 2020 May 1; 24(3):43–57. https://doi.org/10.31272/jeasd.24.3.3

28. Padmaloshani P, Nirmala S. Semi-distributed dynamic inter-cell interference coordination scheme for interference avoidance in heterogeneous networks. ETRI Journal. 2020 Apr; 42(2):175–85. https://doi.org/10.4218/etrij.2018-0362

29. Wang H, Song R, Leung SH. Removal of ICI and IBI in Wireless Heterogeneous Networks With Timing Misalignment. IEEE Communications Letters. 2017 Jan 16; 21(5):1195–8. https://doi.org/10.1109/LCOMM.2017.2652445

30. Fang D, Qian Y, Hu RQ. Security for 5G mobile wireless networks. IEEE access. 2017 Dec 4; 6:4850–74. https://doi.org/10.1109/ACCESS.2017.2779146

31. Elmahi E, Salekzamankhani S, Sharma M. In-Depth Analysis of Signal Jammers' and Anti-Jamming Effect on 5G Signal. In2019 7th International Conference on Future Internet of Things and Cloud Workshops (FiCloudW) 2019 Aug 26 (pp. 1–6). IEEE.

32. Lichtman M, Rao R, Marojevic V, Reed J, Jover RP. 5G NR jamming, spoofing, and sniffing: Threat assessment and mitigation. In2018 IEEE international conference on communications workshops (ICC Workshops) 2018 May 20 (pp. 1–6). IEEE.

33. Han T, Gong J, Liu X, Islam SR, Li Q, Bai Z, et al. On downlink NOMA in heterogeneous networks with non-uniform small cell deployment. IEEE Access. 2018 Jun 8; 6:31099–109. https://doi.org/10.1109/ACCESS.2018.2845440

34. Wen W, Cui Y, Zheng FC, Jin S, Jiang Y. Random caching based cooperative transmission in heterogeneous wireless networks. IEEE Transactions on Communications. 2018 Feb 20; 66(7):2809–25. https://doi.org/10.1109/TCOMM.2018.2808188

35. Abbas ZH, Haroon MS, Abbas G, Muhammad F. SIR analysis for non-uniform HetNets with joint decoupled association and interference management. Computer Communications. 2020 Apr 1; 155:48–57. https://doi.org/10.1016/j.comcom.2020.03.015

36. Peng J, Zeng J, Su X, Liu B, Zhao H. A QoS-based cross-tier cooperation resource allocation scheme over ultra-dense HetNets. IEEE Access. 2019 Feb 24; 7:27086–96. https://doi.org/10.1109/ACCESS.2019.2901506

37. Abbas ZH, Abbas G, Haroon MS, Muhammad F. Analysis of interference management in heterogeneous cellular networks in the presence of wideband jammers. IEEE Communications Letters. 2020 Feb 3; 24(5):1138–41. https://doi.org/10.1109/LCOMM.2020.2971209

38. Haroon MS, Abbas ZH, Abbas G, Muhammad F. Coverage analysis of ultra-dense heterogeneous cellular networks with interference management. Wireless Networks. 2020 Apr; 26(3):2013–25. https://doi.org/10.1007/s11276-019-01965-0

39. Abbas ZH, Abbas G, Haroon MS, Muhammad F, Kim S. Proactive uplink interference mitigation in HetNets stressed by uniformly distributed wideband jammers. Electronics. 2019 Dec 7; 8(12):1496. https://doi.org/10.3390/electronics8121496

40. Błaszczyszyn B, Haenggi M, Keeler P, Mukherjee S. Stochastic geometry analysis of cellular networks. Cambridge University Press; 2018 Apr 19.

41. Muhammad F, Abbas ZH, Li FY. Cell association with load balancing in nonuniform heterogeneous cellular networks: Coverage probability and rate analysis. IEEE Transactions on Vehicular Technology. 2016 Sep 30; 66(6):5241–55. https://doi.org/10.1109/TVT.2016.2614696

42. Zou S, Liu N, Pan Z, You X. Joint power and resource allocation for non-uniform topologies in heterogeneous networks. In2016 IEEE 83rd Vehicular Technology Conference (VTC Spring) 2016 May 15 (pp. 1–5). IEEE.

43. Jiang X, Zheng B, Zhu WP, Wang L, Zou Y. Large system analysis of heterogeneous cellular networks with interference alignment. IEEE Access. 2018 Jan 30; 6:8148–60. https://doi.org/10.1109/ACCESS.2018.2799626

44. Lichtman M, Poston JD, Amuru S, Shahriar C, Clancy TC, Buehrer RM, et al. A communications jamming taxonomy. IEEE Security & Privacy. 2016 Feb 3; 14(1):47–54. https://doi.org/10.1109/MSP.2016.13

45. Qasim M, Haroon MS, Imran M, Muhammad F, Kim S. 5G cellular networks: Coverage analysis in the presence of inter-cell interference and intentional jammers. Electronics. 2020 Sep 20; 9(9):1538. https://doi.org/10.3390/electronics9091538

46. Arif M, Wyne S, Navaie K, Haroon MS, Qureshi S. Clustered jamming in aerial HetNets with decoupled access. IEEE Access. 2020 Aug 4; 8:142218–28. https://doi.org/10.1109/ACCESS.2020.3014119

47. Hernandez-Aquino R, Zaidi SA, McLernon D, Ghogho M. Modelling and performance evaluation of non-uniform two-tier cellular networks through Stienen model. In2016 IEEE International Conference on Communications (ICC) 2016 May 22 (pp. 1–6). IEEE.

48. Abbas ZH, Haroon MS, Muhammad F, Abbas G, Li FY. Enabling soft frequency reuse and Stienen's cell partition in two-tier heterogeneous networks: Cell deployment and coverage analysis. IEEE Transactions on Vehicular Technology. 2020 Dec 29; 70(1):613–26. https://doi.org/10.1109/TVT.2020.3048090

49. Ullah A, Abbas ZH, Abbas G, Muhammad F, Jiao L. Performance analysis of user-centric SBS deployment with load balancing in heterogeneous cellular networks: A Thomas cluster process approach. Computer Networks. 2020 Apr 7; 170:107120. https://doi.org/10.1016/j.comnet.2020.107120